Esterified Coconut Coir by Fatty Acid Chloride as Biosorbent in Oil Spill Removal

Nor Azah Yusof,[a,b,*] Hayati Mukhair,[b] Emilia Abd. Malek,[b] and Faruq Mohammad [a]

Coconut coir, an agricultural waste, was chemically modified using esterification by fatty acid chloride (oleoyl chloride and octanoate chloride) for oil spill removal purposes. The modified coir (coir-oleate and coir-octanoate) were characterized by spectroscopy, thermal studies, contact angle, and morphological studies. The modified coir exhibited an enhancement towards the hydrophobic property but a decreased thermal stability. The oil adsorption performance was tested using a batch adsorption system. The effect of sorbent dosage, oil concentration, and effect of adsorption time on the adsorption capacity of the modified coir were also studied. From the analysis, the long chain oleoyl chloride (C18) was shown to be a better modifier compared to octanoate chloride (C8). The isotherm study indicated that the oil adsorption fitted well to a Langmuir model rather than Freundlich model. From the kinetic study, the result revealed a good fit in pseudo-second order model for all samples studied. The study therefore suggests that esterified coconut coir can serve as a potential biomaterial for the adsorption of spilled oil during operational failures.

Keywords: Modified coconut coir; Esterification; Natural fiber; Oil spill

Contact information: a: Institute of Advance Technology (ITMA), Universiti Putra Malaysia, 43400 Serdang, Selangor, Malaysia; b: Department of Chemistry, Universiti Putra Malaysia, 43400 Serdang, Selangor, Malaysia;
** Corresponding author: azahy@upm.edu.my; Tel.: +6-03-8946-6782; Fax: +6-03-8943-5380.*

INTRODUCTION

In recent years the contamination of sea water by oil spills has attracted a great deal of interest, and such interest was heightened due to the latest tragic incident that occurred in the Gulf of Mexico on the British Petroleum (BP)-operated Macondo Prospect. For such incidents in general, the water pollution caused by the oil spill leaves damage to the quality of human health and the environment, disturbs the marine life ecosystem, in addition to causing serious adverse economic impact on the life of people depended on fisheries, agriculture, and tourism (Lim and Huang 2007). The main reasons for these oil spills at sea are human mistakes and carelessness of daily activities during the oil drilling operations, oil storage tankers, runoff from offshore oil explorations and productions, and spills from tanker loading and unloading operations (Li *et al*. 2013). By keeping in view the serious impacts due to oil spill-resultant water contamination, it is therefore very important to remediate the spilled oil as quickly as possible to avoid further damage to the ecosystem.

Some commercial methods for oil spill treatment such as booms, dispersants, skimmers, oil-water separators, and sorbent materials have been developed; however, a majority of these approaches are either costly or less environmental friendly or both. For example, the use of dispersants during oil spill treatment generates toxic reactions that may fail to balance the life in the ecosystem due to the usage of harmful chemicals linked to this process. In some methods, the treatment may cause the oil to sink by increasing its density, which makes the oil difficult to collect (Chapman *et al*. 2007).

Besides these, the use of sorbents for oil spill removal has the advantages of making the oil separation process in an economical, efficient, and environmental friendly way; however, the use of this approach during the cases where thick layers of floating oils needs to be removed still remains a challenge (which is ideal for use of a skimmer and density-based separation) (Hubbe *et al.* 2013). In general, the sorbent materials synthesized from non-renewable petroleum based sources are widely used in floating booms for the containments assortment and for the collection of spilled oils. During this process, the addition of sorbent material concentrates and transforms the liquid oil to semi-isolid phase that can be removed easily from the surface of water (Adebajo and Frost 2004; Ali *et al*. 2012). They can be used to recover the oil through the mechanisms of absorption, adsorption or both. The other benefit of using a sorbent is its ease of handling, fast oil uptake, and the capability to capture and retain oil for retrieval at a later time (Parab *et al*. 2010).

Generally, the three major classes of oil sorbents include the inorganic mineral products, organic synthetic products, and organic natural products. Recently, the commercial sorbents that are widely used contains organic synthetic products such as polypropylene (PP) and polyurethane due to their oleophilic-hydrophobic properties (Lim and Huang 2007). However, the limitation for this sorbent material is that they are non-biodegradable and can be difficult to handle after their usage. The mineral products used in oil sorbents include perlite, vermiculite, and diatomite, as most of them have low buoyancy and oil sorption capacity (Warr *et al*. 2009). Thus, due to the limited availability of synthetic organic and mineral product sorbents, many researchers have embarked on a quest for alternative natural sorbent materials derived from agricultural waste products as a sorbent for oil spill treatment purposes.

Lignocellulose (mainly celluloses, hemicelluloses, and lignin) constitutes a renewable raw material that is widely available in the form of waste from agricultural residues such as sugarcane bagasse, cereal straw, peat moss, wool, rice hulls, coconut coir, and corn cob (Lundqvist *et al*. 2002). Because lignocellulose has high oil adsorption capacity, and is biodegradable, renewable, environmental friendly, inexpensive, and is easily available, it has been a subject of interest among researchers to further reveal its capability as oil sorbents. The organic sorbents can adsorb the oil up to 15 times their weight, but the limitation of these materials is their tendency to adsorb both water as well as oil, causing them to sink. This happens due to the presence of the hydroxyl group in the cellulose and hemicelluloses on the polymer backbone. This particular functional group is responsible mainly for the hygroscopic properties of lignocellulosic materials and these defects can however be reduced considerably by some chemical modification. One approach is by the replacement of the hydroxyl functional group from cellulose, hemicelluloses, and lignin present at the polymeric backbone with more hydrophobic groups by means of chemical reactions (Sun *et al*. 2004).

One form of lignocellulose material, coconut coir, is a fibrous layer outside the coconut shell and is one of the largest waste products of the copra industry. Coir is used in manufacturing of soil-treatment fibers, rope, and doormats around the world. Although coconut coir has been commercially available for many years, its capability as oil sorbent is still limited. Therefore, herein we chose coconut coir as a model biosorbent and studied its potential for removing oil from water. We carried out the esterification of coir by using fatty acid chloride in order to increase the oil adsorption capacity and to increase the hydrophobic properties of the material. Thus, chemically treated coir was thoroughly characterized by Fourier transform infrared spectroscopy (FTIR), Field emission scanning electron microscopy (FESEM), thermal analysis, and static contact angle measurements. In addition, the oil adsorption studies were carried

out to determine changes in sorbed amounts and adsorption rates. The system was further analyzed relative to kinetic studies and isotherm models.

EXPERIMENTAL

Biosorbent Preparation

The coconut coir raw material used in this study originated from Sungai Tengi Kiri Village, Selangor, Malaysia. The raw coir was ground into small and short shapes in a high speed grinder, and the visible dust/impurities were removed by washing and boiling with distilled water. Following this, the fiber was washed several times with acetone before drying in the oven at 60 °C overnight. To ensure the freshness of the raw materials, no further treatment was carried out.

Esterification of Coir by Fatty Acid Chloride

The esterification reaction of coir was carried out in a reflux setup maintained under a fume hood. For that, approximately 5 g of coir was weighed and placed in a 250 mL three necked round bottom flask. To this, 100 mL of 1% (v/v) N-bromosuccinimide (NBS) catalyst prepared in a DMaC/LiCl solvent system was added and heated up to 100 °C with stirring. To this mixture, 10% (v/v) concentration of oleoyl chloride was added drop-wise, and the reaction was allowed to proceed continuously for 4 h under the same conditions of temperature and stirring. After the period during which the esterification process was completed, the acylated fiber was filtered and washed with a series of solvents including toluene, ethanol, water, and acetone to remove any unreacted oleoyl chloride and unwanted byproducts. Then the fiber was dried to a constant weight in an oven at 70 °C. The same synthetic process was repeated for the esterification of the coir by means of octanoyl chloride.

Oil Adsorption Study

The adsorption study was carried out in a batch system, and for that, the crude oil (engine oil) was mixed with 100 mL of water and stirred for 5 min at 120 rpm at room temperature. After the stirring, when oil was observed to be floating as a layer on the water surface, the modified coir (formed from 30% oleoyl chloride) was added to the oil/water mixture. The mixture was then shaken for 5 min at room temperature and the modified coir was then removed from the mixture using a mesh screen and drained for 1 min. The oil sorption capacity (Q, g-oil/g-sorbent) was calculated according to Wang *et al.* (2013), as shown in Eq. 1,

$$Q = \frac{M_a - M_i - M_w}{M_i} \quad (1)$$

where M_a (g) is the weight of wet modified coir after the adsorption, M_i (g) is the initial weight of modified coir, and M_w is the weight of water adsorbed by the modified coir. The amount of water adsorption was determined by the extraction-separation method using n-hexane as a solvent. All the tests were done in triplicates.

Instrumental Analysis

The functional group analysis in raw coir and esterified coir was performed by using FTIR spectroscopy (Perkin Elmer Spectrum 100 Series), and the spectra were recorded in the range of 400 to 4000 cm^{-1} wavenumbers. The thermal stability of the

modified coir was determined by thermogravimetric (TGA) and derivative thermogravimetric (DTG) analyses, where the sample weight loss was monitored as a function of temperature by making use of Perkin-Elmer Thermogravimetry Analyzer TGA7. The samples were analyzed in a temperature range of 25 to 600 °C and at a heating rate 10 °C/min with nitrogen flow rate of 50 mL/min. For analyzing the surface morphology of the samples, a field emission scanning electron microscope model LEO 1455 VPFESEM was used. The sample surface was coated with gold by a Bio-rad coating system, and the scanning electron micrographs (SEM) were recorded at a magnification of 10000X. The static contact angle measurements were used to identify the solid-liquid phase interactions between sorbents and water. In this study, video contact angle ganiometer (vca 3000s) from Vistec Technology was used to analyze the samples.

RESULTS AND DISCUSSION

Physical Observation of Modified Coconut Coir

The hydrophobicity of the modified coir was initially evaluated by immersing it into a two immiscible solvent mixture of water (bottom) and hexane (top). The set-up is shown in Fig. 1. As one can see from the figure, the raw coir tended to be more homogenous in the water phase than in hexane, and this is attributable to the presence of hydroxyl groups at the polymer's backbone, which by means of hydrogen bonding tends to be dispersible in water. The same coir on chemical modification, *i.e.* coir-oleate exhibited a more hydrophobic character as indicated by its migration and tendency to get remain in the hexane phase. The observation of such property may be due to the formation of hydrophobic ester bonds onto the coir by the substitution of hydroxyl groups of the polymer backbone. However, with an increase in the concentration of oleoyl chloride, the homogeneity of coir-oleate tended to be decreasing, *i.e.* the 10% oleoyl chloride product was more homogeneous in hexane phase than the corresponding 20% and 30% oleoyl chloride reaction products. The reason for this decreased homogeneity is likely due to the increased carbon content by means of esterification onto the surface of coir polymer, thereby promoting for the precipitation in the same hexane phase with a greater rate in the case of the 30% oleoyl chloride (Fig. 1d) than the 20% oleoyl chloride product (Fig. 1c). Similarly, the octanoate modified coir (Fig. 1e) also dispersed in hexane phase through the formation of hydrophobic octanoic groups and the presence of short chain C8 (compared to long chain oleoly of C18) surface groups is the reason for its dispersity in hexane solvent without any precipitation.

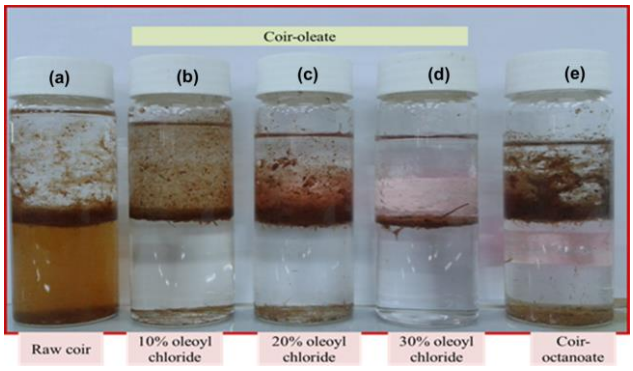

Fig. 1. Effect of fatty acid chloride concentration towards the hydrophobic character of coir where (a) raw coir, (b) coir-oleate with 10% oleoyl chloride, (c) coir-oleate with 20% oleoyl chloride, (d) coir-oleate with 30% oleoyl chloride, and (e) coir-octanoate

FTIR Analysis of the Modified Coir

The FTIR spectroscopic analysis was performed so as to determine the nature of chemical bonding in raw coir and the modified coirs (coir-oleate). The FTIR spectra of raw coir and coir-oleate when treated with different oleoyl chloride concentrations, different NBS concentration, and different reaction temperatures are illustrated in Figs. 2, 3, and 4, respectively.

Effect of oleoyl chloride concentration

The comparison of FTIR spectra of raw coir with those of coir-oleate (various concentrations) and coir-octanoate is shown in Fig. 2(a-e). From the figure, the presence of absorption peaks at 3372 cm^{-1}, 2914 cm^{-1}, 1638 cm^{-1}, 1385 cm^{-1}, 1241 cm^{-1}, and 1068 cm^{-1} in the raw coir (Fig. 2a) spectrum was associated with raw coconut coir. The broad peak at 3372 cm^{-1} originated from O-H stretching of the hydroxyl group. The narrowing of hydroxyl band around 3374 to 3329 cm^{-1} for the treated coir samples (Fig. 2b-2d) suggests the occurrence of partial esterification. In general, the broadness of hydroxyl band around 3300 to 3500 cm^{-1} is related to the inter- and intra-molecular hydrogen bonding in polysaccharides; it can be concluded from the present case that the narrowing of this band is also attributable to a lower degree of hydrogen bonding (Calado *et al.* 2000). Similarly, the peak around 2914 cm^{-1} indicates the asymmetric and symmetric stretching vibration of CH_2 and CH_3, and the strong band at 1068 cm^{-1} is attributed to C-O stretching in cellulose, hemicelluloses, and lignin (Rana *et al*. 1996). The peak at 1457 cm^{-1} in the raw coir represents the aromatic C=C stretch of aromatic ring of lignin, and the bands at 1241 cm^{-1} and 1385 cm^{-1} are assigned to the C-O and C-H bending vibrations respectively (Wang *et al.* 2013). The peak at 1638 cm^{-1} can be assigned to C=C alkene stretching of lignocelluloses material.

After the modification reaction, the existence of (C=O) carbonyl ester peak in coir-oleate FTIR spectra at 1729 cm^{-1} indicates that the esterification had occurred. Besides that, the decrease in (O-H) hydroxyl peak intensity also showed that some of the hydroxyl groups were substituted by long chain acyl groups. As the concentration of oleoyl chloride increased, the vibration signal of C=O ester showed higher intensity and is an indication of a formation of more ester bonds. The high intensity of CH_2 and CH_3 peaks at 2915 cm^{-1} also indicates an increase of alkyl groups in coir-oleate. The coir-octanoate (Fig. 2e) showed a low vibration signal of C=O compared to coir-oleate, an indication of a low concentration of coir ester product being formed.

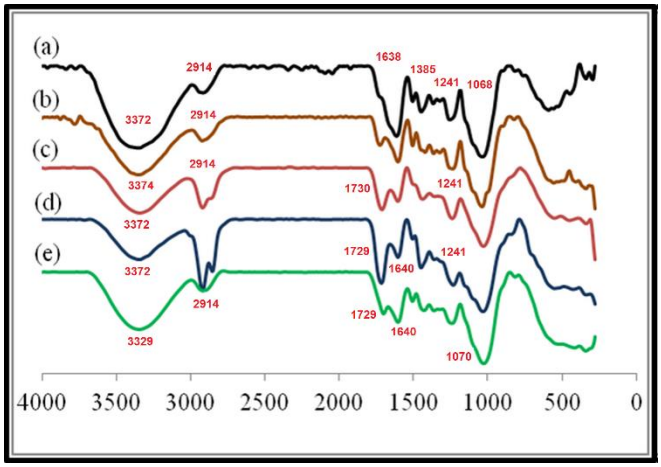

Fig. 2. FTIR spectra of (a) raw coir, (b) coir-oleate in 10% (v/v) oleoyl chloride, (c) coir-oleate in 20% (v/v) oleoyl chloride, (d) coir-oleate in 30% (v/v) oleoyl chloride, and (e) coir-octanoate in 10% (v/v) octanoate chloride

Effect of N-bromosuccinimide (NBS) catalyst concentration

The comparison of the FTIR spectra of coir-oleate towards NBS concentration is shown in Fig. 3(a-d). From the figure, the NBS's concentration was observed to have some effect on the esterification of coir, *i.e.* as the concentration of NBS reached 3% (w/v), the C=O carbonyl ester peak at 1739 cm^{-1} became intense when compared to reaction carried without the NBS catalyst (Fig. 3a). Besides that, the intense peak of C-H alkyl group around 2915 cm^{-1} in Fig. 3d also indicates the increase of alkyl groups after the coir's modification reaction.

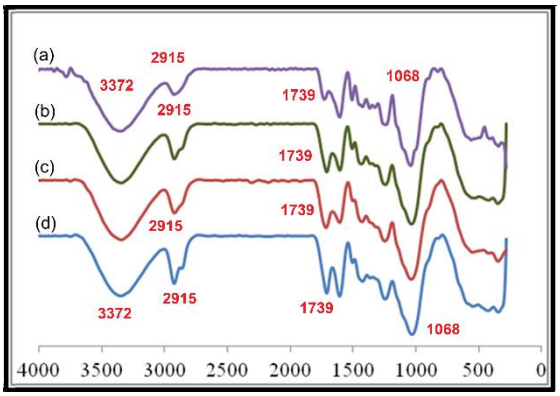

Fig. 3. FTIR spectra of (a) coir-oleate without catalyst, (b) coir-oleate in 1% (w/v) of NBS, (c) coir-oleate in 2% (w/v) of NBS and (d) coir-oleate in 3% (w/v) of NBS catalyst

Effect of reaction temperature

The FTIR spectrum of coir-oleate formed from different reactions, *i.e.* the effect of reaction temperature towards degree of esterification is shown in Fig. 4(a-b). It can be concluded from the Fig. 4a that the occurrence of esterification reaction was better achieved at higher temperature (70 to 90 °C) compared to the reaction at room temperature, as observed by an intense absorption peak at 1730 cm^{-1} and a narrower peak of hydroxyl band around 3400 cm^{-1}.

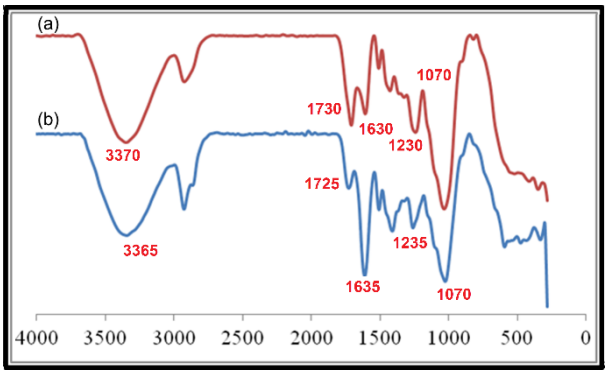

Fig. 4. FTIR spectra of coir-oleate at (a) 70-90˚C and (b) room temperature

Thermal Analysis

The TGA and DTG thermograms in Fig. 5(a-d) show the mass change of raw coir and coir-oleate that was synthesized by using different oleoyl chloride (10%, 20%, and 30%) v/v concentrations. It can be seen clearly from the figure that the thermal stability of oleoylated fibre became slightly decreased upon chemical modification by esterification. The unmodified coir started decomposition (significant weight loss and phase change) at 270°C (Fig. 5a), whereas the decomposition temperatures for the modified coirs were shifted to lower values of around 177.65 °C, 171.6 °C and 167.19 °C

for the 10%, 20% and 30% oleoyl chloride concentration (respectively). This decrease in temperatures is an indication that the decomposition rate (loss of weight against time and temperature) of esterified coir samples was faster than that of the corresponding unmodified coir. The faster decomposition of the modified coirs can be attributed to the lack of hydrogen bonding in the formed esterified products from the substitution of the hydroxyl groups of raw coir with long chain acyl groups. This behaviour is also attributed to a decrease in the crystallinity associated with an esterification reaction (Freire *et al*. 2006).

There are two major degradation steps that can be seen in thermograms for all samples studied, the first degradation step which occur around 167 °C to 200 °C in Fig. 5(b, c and d) is assigned to the esterification fraction, where the breakage of ester bond and this particular peak is absent for the raw coir sample shown in Fig. 5(a). Second, the degradation step at high temperature seen around 353.58 °C for raw coir (a), 333.89 °C for 10% coir-oleate (b), 335 °C for 20% coir-oleate (c), and 348 °C for 30% coir-oleate (d) is attributed to the raw polymer backbone and more the rigid component such as lignin (Jandura *et al*. 2000).

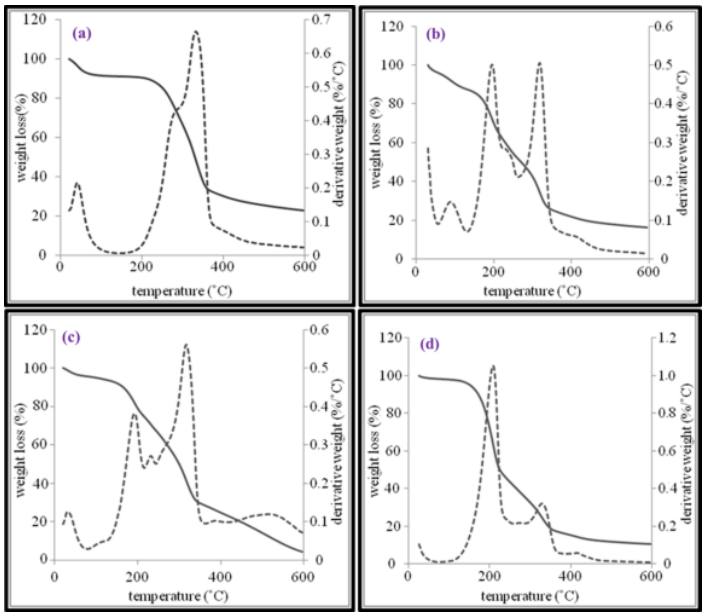

Fig. 5. TGA and DTG thermograms of (a) raw coir, (b) coir-oleate 10%, (c) coir-oleate 20%, and (d) coir-oleate 30%.

Surface Morphology

The morphology and surface structure of raw coir, coir-oleate, and coir-octanoate were analyzed by FESEM with magnification of 10000, as shown in Fig. 6(a-c).

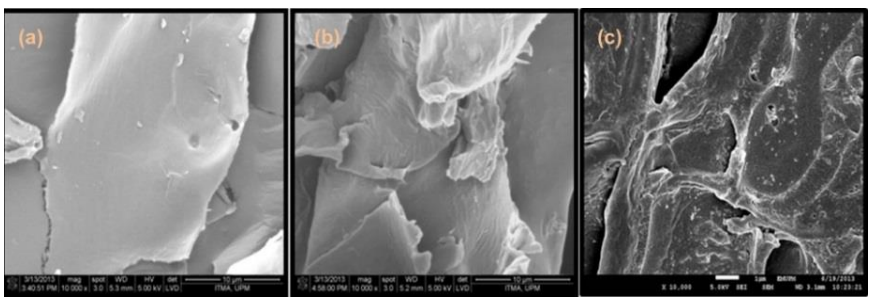

Fig. 6. FESEM micrographs of (a) raw coir, (b) coir-oleate (formed from 30% oleoyl chloride), and (c) coir-octanoate

It can be seen clearly from the figure that the raw coir had a smooth surface, which further changed to rough on modification by esterification. The coir-octanoate seems to be even darker and rougher when compared to the raw coir and coir-oleate. This change in morphology of raw coir is favorable for the retention of oil in coir assembly, thus providing more oil storage (Sidik *et al*. 2012).

Static Contact Angle

Figure-7(a-e) shows the static contact angle for the raw coir, coir-oleate (various concentrations), and coir-octanoate. From the analysis of results, the contact angle between coir and water increased from 66.9° to 85.8° with an increase of oleoyl chloride concentration used for esterification. This indicates that the oleoylated coir fiber had more hydrophobic character than the raw coir due to long chain acyl group bonded to the fiber backbone (Li *et al*. 2013). Therefore, it can be concluded that the oleophilic-hydrophobic characteristics of the modified coir increased greatly after esterification. However, the contact angle for coir-octanoate was slightly decreased and gave no significant difference in hydrophobicity compared to raw coir. The observation of this property may be due to the inability of the formed octanoic groups to exhibit a dominant hydrophobic effect due to its C8 short chain compared to the corresponding C18 long chain oleoyl groups formed by the replacement of hydroxyl groups of polymer backbone.

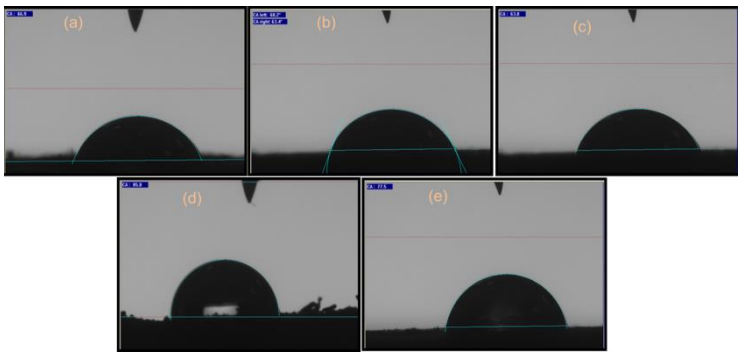

Fig. 7. Static contact angle of (a) raw coir (66.9°), (b) coir-oleate with 10% oleoyl chloride (68.2°), (c) coir-oleate with 20% oleoyl chloride (77.5°), (d) coir-oleate with 30% oleoyl chloride (85.8°), and (e) coir-octanoate with 10% octanoate chloride (63.8°)

Oil Adsorption Studies

Effect of sorbent dosage

The effect of adsorbent dosage on the amount of crude oil removal was studied by using the sorbent mass between 0.2 g and 1 g, and results are shown in Fig. 8(a-b). As shown in the figure, the amount of raw coir, coir-oleate (formed from 30% oleoyl chloride), and coir-octanoate in oil/water solution was observed to greatly affect the oil uptake and the rate of percentage removal of oil found to be increased with an increase in the amount of sorbent used. An amount of 0.6 g of coir-oleaote was able to remove all 100% of the oil, in contrast to the coir-octanoate and raw coir (Fig. 8a). In contrast, the adsorption capacity of sorbent decreased with increasing sorbent dosage for all the samples studied, and the maximum adsorption capacity was found to be 36.46 (w/w) when 0.2 g of coir-oleate was used. This increased the amount of oil adsorption with that of sorbent dosage due to the availability of greater number of active sites on the surface of coir (by means of acyl containing long chain groups) for the crude oil to be adsorbed, thus leading to a higher interaction between the hydrophobic oil molecules and the adsorbent (Arief *et al*. 2008). However, the decreased adsorption capacity with

the sorbent amount is basically due to the higher unsaturated adsorption sites still left after the adsorption process (Wan Ngah and Hanafiah 2008).

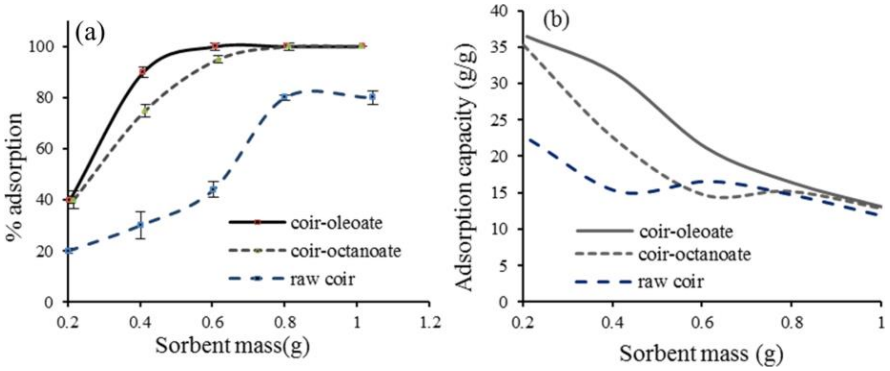

Fig. 8. Effect of sorbent dosage on (a) percent of adsorption and (b) adsorption capacity (oil volume 10 mL, exposed oil 15 min, 25°C)

Effect of contact time on oil sorption and kinetics studies

The effect of contact time on the oil sorption of raw coir, coir-oleate, and coir-octanoate is shown in Fig. 9. The oil sorption capacity was high for coir-oleate in comparison to the coir-octanoate and raw coir, and this value slightly increased with that of the increased contact time for all the samples. The adsorption process seemed to occur rapidly during the first 2 min followed by a relatively slow oil uptake before it reached an equilibrium state; the further increase of time slowed down the process due to the availability of a limited number of sites for the oil to get adsorbed. These results also showed that the sorbents displayed a fast adsorption property toward the oil as indicated by the observation of only a small difference of sorption capacity between the initial and final sorption volumes. This observation is in agreement with the findings by Wang *et al*. (2013).

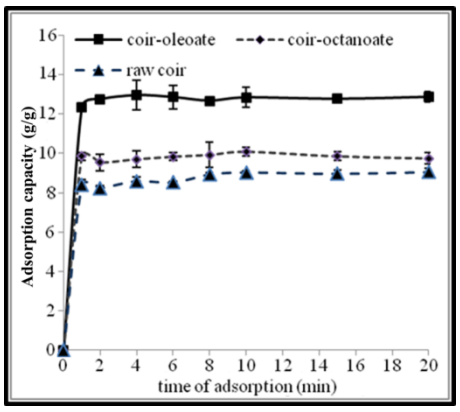

Fig. 9. Effect of adsorption time on oil sorption capacity (adsorbent dosage: 0.2 g)

To understand the sorption process, the experimental data were further analyzed according to two types of kinetic models, the pseudo-first-order and pseudo-second-order models (Fig. 10), as represented in linear forms by Eqs. 2 and 3,

$$\log(Q_e - Q_t) = \log Q_e - \frac{k_1 t}{2.303} \quad (2)$$

$$\frac{t}{Q_t} = \frac{1}{k_2 Q_e^2} + \frac{t}{Q_e} \quad (3)$$

where Q_e (g/g) and Q_t (g/g) are the amount of oil adsorbed at equilibrium and at time t (min), respectively, and k_1 is the rate constant of pseudo-first order adsorption, while k_2 is the rate constant of pseudo-second order adsorption. The linear regression coefficient of determination, R^2 and parameters of kinetic models were calculated and are listed in Table 1. From the analysis, the results indicate that the data fit well with pseudo-second order model with R^2 values higher than 0.999. The experimental $Q_{e\ exp}$ and theoretical $Q_{e\ calc}$ values are agreeable to each other as compared against the pseudo-first order model. Therefore, the adsorption behavior of oil by raw coir, coir-oleate, and coir-octanoate predominantly followed the pseudo-second order kinetic model.

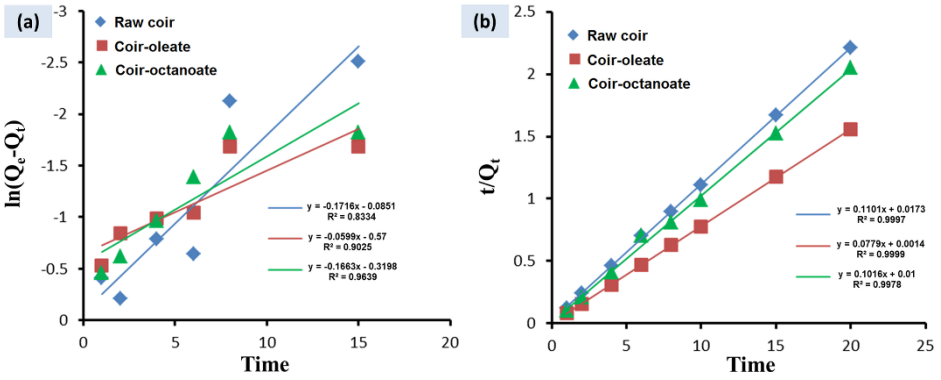

Fig. 10. Comparison of (a) pseudo first order and (b) pseudo second order rate equation model for raw coir, coir-oleate, and coir-octanoate

Table 1. Sorption Parameters of Pseudo-First-Order and Pseudo-Second-Order Kinetic Models

	Pseudo - first order				Pseudo - second order		
	$Q_{e\ exp}$ (g/g)	$Q_{e\ calc}$ (g/g)	k_1 (g/g min)	R^2	$Q_{e\ calc}$ (g/g)	k_2 (g/g min)	R^2
Raw coir	9.20	1.07	0.393	0.833	9.14	1.74	0.997
Coir-oleate	12.27	0.24	0.366	0.902	12.38	3.23	0.999
Coir-octanoate	9.40	0.49	0.382	0.963	9.56	7.62	0.997

Effect of initial oil concentration and isotherm studies

The effect of initial oil concentration adsorbed onto the coir surface was studied at different initial oil concentrations ranging from 0.05 to 0.2 % (mL/mL). As shown in Fig. 11(a), the percentage adsorption of oil onto the coir was found to be decreased with an increase of initial oil concentration. Also, the coir-oleate and coir-octanoate showed 100% of oil removal at maximum 0.10 mL mL^{-1} and started to decrease when the oil concentration is 0.12 mL mL^{-1} and above, while the raw coir can only adsorb the oil at a maximum concentration of 0.05 mL mL^{-1}. From Fig. 11(b), the adsorption capacity seems to have increased with an increase of initial concentration and to have reached to its equilibrium stage at the initial concentration of 0.2 mL mL^{-1}. This result showed that as the initial oil concentration increases, the active sites on coir, coir-oleate, and coir-octanoate become saturated and hence the excess oil cannot get adsorbed by the adsorbent, which further leads to a decrease in the percentage of oil removal. The modified coir (coir-oleate and coir-octanoate) showed higher performances compared to the raw coir due to the existence of the same long chain acyl groups on polymer backbone which gives more active sites for the sorption process by reducing its hydrophilic ability.

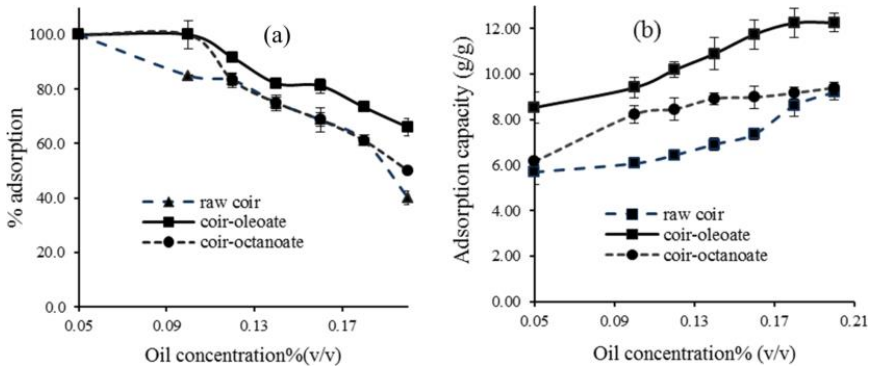

Fig. 11. Effect of oil concentration towards (a) percentage of removal (b) adsorption capacity (sorbent mass 0.6 g, room temperature, exposed to oil 15 min)

An isotherm study is a fundamental aspect in determining the nature of adsorption between the adsorbent and adsorbate; it indicates how the oil gets distributed between sorbents at equilibrium. The two types of isotherm models chosen for this study includes the Langmuir isotherm model (Fig. 12a) and the Freundlich isotherm model (Fig. 12b). The Langmuir isotherm assumes that only one monolayer of adsorbate molecule can be adsorbed on the surface with no transmigration of adsorbate in the plane of surface (Wang *et al*. 2013). The linear form of Langmuir isotherm is given in Eq. 4 as,

$$\frac{C_e}{Q_e} = \frac{1}{(b \times Q_m)} + \frac{C_e}{Q_m} \qquad \text{(Langmuir isotherm model)} \qquad (4)$$

where C_e (g/mL) is the equilibrium concentration of the adsorbate, Q_e (g/g) is the amount of adsorbate adsorbed per unit mass of adsorbent, b is the Langmuir coefficient related to the affinity between adsorbent and adsorbate, and Q_m (g/g) is the maximum monolayer adsorption capacity.

The Freundlich isotherm model assumes heterogeneous surface energies, and a heterogeneous adsorption surface that has unequal number of available sites with different adsorption energies. This model describes the adsorption onto heterogeneous sites of adsorbent involving multilayer adsorption. The Freundlich isotherm equation is represented in Eq. 5 as,

$$\ln Q_e = \ln K_f + \frac{1}{n} \ln C_e \qquad \text{(Freundlich isotherm)} \qquad (5)$$

where K_f is the Freundlich constant related to the adsorption capacity, and the slope $1/n$ ranging between 0 to 1 is indicator of adsorption intensity and surface heterogeneity, which is more heterogeneous as its value gets closer to 0.

The parameters of the Langmuir and Freundlich models such as isotherm constants and coefficients of determination (R^2) are listed in Table 2. From the results, the coefficients of determination R^2 values for Langmuir isotherm model were closer to 1 for all the samples studied as compared against the values of Freundlich isotherm model. Furthermore, the difference between calculated Q_m values and the experimental values Q_e for the Langmuir model were closer to each other, meaning that the adsorption data for the coir, coir-oleate and coir-octanoate could be better described by the Langmuir isotherm model than the corresponding Freundlich model. Therefore, it can be assumed that the monolayer adsorption occurred on a homogeneous surface where there is no interaction between the adsorbed molecules on the neighboring sites (Ibrahim *et al*. 2010).

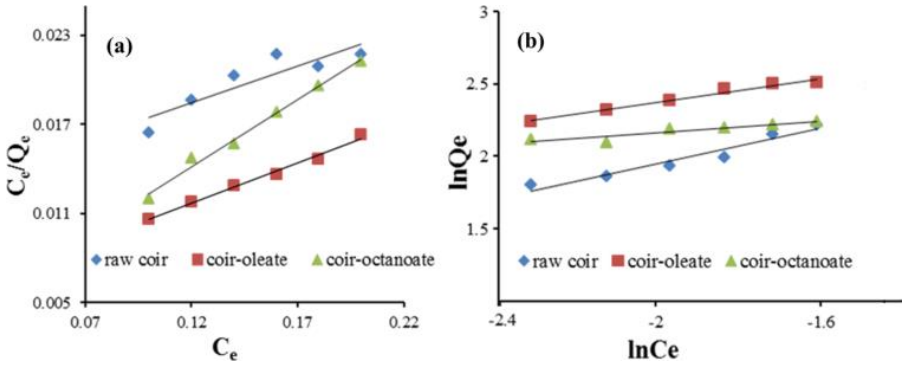

Fig. 12. (a) Langmuir and (b) Freundlich isotherm models for the raw coir, coir-oleate, and coir-octanoate

Table 2. Parameters of the Langmuir and Freundlich Models and Coefficients of Determination for the Sorption of Oil by (a) Raw Coir, (b) Coir-oleate, and (c) Coir-octanoate

	Langmuir model				Freundlich model			
	Q_e (g/g)	Q_m (g/g)	b (mL/g)	R^2	Q_e (g/g)	K_f (mL/g)	$1/n$	R^2
(a)	9.20	11.29	0.0119	0.8039	23.93	14.1739	2.9958	0.9397
(b)	12.27	15.31	0.2624	0.9900	24.47	19.3211	3.4953	0.9751
(c)	9.40	11.96	0.2828	0.9902	12.98	15.5473	3.3189	0.8461

CONCLUSIONS

1. Coconut coir was successfully esterified using oleoyl chloride by the replacement of the hydroxyl groups of polymer backbone with that of the acyl groups so as to achieve sufficient hydrophobic behavior to interact highly with the similarly hydrophobic oil molecules.
2. It was found that with an increase of oleoyl chloride concentration during esterification, the hydrophobic character of the formed coir-oleate was increased and at the same time, the precipitation rate in hexane also increased due to an increase in the content of carbon onto the surface of the coir. This fast precipitation property is especially important for oil-spill removal applications due to the fact that a highly stable and homogenous coir can make the extraction process to be difficult to separate after the oil adsorption (from the oil-water solvent system).
3. The presence of esterified bonds onto the coir, the effect of NBS, and the effect of temperature towards the esterification were confirmed by the FTIR analysis.
4. When tested for oil adsorption studies, the oleoyl esterified coir (30%) was found to have a better oil adsorption performance than the corresponding unmodified coir and octanoate-modified coir. This enhanced oil adsorption property can be explained by the amount of carbon content and resulting hydrophobic property from the analysis of static angle measurements, where the coir-oleate (C18) has a very high contact angle against water surface than the corresponding unmodified coir and coir-octanoate (C8).

5. The kinetic reaction studies indicated that the oil adsorption by the coir-oleate followed the pseudo-second order kinetics, where the rate of reaction depends on both the parameters of oil concentration and the sorbent.
6. Further, the isotherm studies indicate that the adsorption followed the Langmuir isotherm model involving only a homogeneous monolayer surface for the adsorption of oil.
7. Based on the findings, it can be concluded that the coir-oleate can serve as an alternative for oil spill and wastewater problem due to its easy modification, abundance and biodegradability.

ACKNOWLEDGMENTS

The authors are grateful for the financial support in terms of Graduated Research Fellowship (GRF) from Universiti Putra Malaysia (UPM) and Ministry of Education Malaysia to carry out this research.

REFERENCES CITED

Adebajo, M. O., and Frost, R. L. (2004). "Acetylation of raw cotton for oil spill cleanup application : An FTIR and 13C MAS NMR spectroscopic investigation," *Spectrochim. Acta A Mol. Biomol. Spectrosc.* 60(10), 2315-2321. DOI:10.1016/j.saa.2003.12.005

Ali, I., Asim, M., and Khan, T. A. (2012). "Low cost adsorbents for the removal of organic pollutants from wastewater," *J. Environ. Manage.* 113(2012), 170-183. DOI:10.1016/j.jenvman.2012.08.028

Arief, V. O., Trilestari, K., Sunarso, J., Indraswati, N., and Ismadji, S. (2008). "Recent progress on biosorption of heavy metals from liquids using low cost biosorbents: Characterization, biosorption parameters and mechanism studies," *Clean Soil Air Water* 36(12), 937-962. DOI:10.1002/clen.200800167

Calado, V., Barreto, D. W., and D'Almeida, J. R. M. (2000). "The effect of a chemical treatment on the structure and morphology of coir fibers," *J. Mater. Sci. Lett.* 19(23), 2151–2153. DOI: 10.1023/A:1026743314291

Chapman, H., Purnell, K., Law, R. J., and Kirby, M. F. (2007). "The use of chemical dispersants to combat oil spills at sea: A review of practice and research needs in Europe," *Mar. Pollut. Bull.* 54(7), 827-838. DOI:10.1016/j.marpolbul.2007.03.012

Freire, C. S. R., Silvestre, A. J. D., Neto, C. P., Belgacem, M. N., and Gandini, A. (2006). "Controlled heterogeneous modification of cellulose fibers with fatty acids : Effect of reaction conditions on the extent of esterification and fiber properties," *J. Appl. Polym. Sci.* 100(2), 1093-1102. DOI:10.1002/app.23454

Hubbe, M. A., Rojas, O. J., Fingas, M., and Gupta, B. S. (2013). "Cellulosic substrates for removal of pollutants from aqueous systems: A Review. 3. Spilled oil and emulsified organic liquids," *BioResources* 8(2), 3038-3097. DOI: 10.15376/biores.8.2.3038-3097

Ibrahim, S., Wang, S., and Ang, H. M. (2010). "Removal of emulsified oil from oily wastewater using agricultural waste barley straw," *Biochem. Eng. J.* 49(1), 78-83. DOI:10.1016/j.bej.2009.11.013

Jandura, P., Riedl, B., and Kokta, B. V. (2000). "Thermal degradation behavior of cellulose fibers partially esterified with some long chain organic acids," *Polym.*

Degrad. Stabil. 70(3), 387-394. DOI:10.1016/S0141-3910(00)00132-4

Li, D., Zhu, F. Z., Li, J. Y., Na, P., and Wang, N. (2013). "Preparation and characterization of cellulose fibers from corn straw as natural oil sorbents," *Ind. Eng. Chem. Res.* 52 (1), 516-524. DOI: 10.1021/ie302288k

Lim, T., and Huang, X. (2007). "Evaluation of kapok (*Ceiba pentandra* (L.) Gaertn.) as a natural hollow hydrophobic-oleophilic fibrous sorbent for oil spill cleanup," *Chemosphere* 66(5), 955-963. DOI:10.1016/j.chemosphere.2006.05.062

Lundqvist, J., Teleman, A., Junel, L., Zacchi, G., Dahlman, O., Tjerneld, F., and Sta, H. (2002). "Isolation and characterization of galactoglucomannan from spruce (*Picea abies*)," *Carbohyd. Polym.* 48(1), 29-39. DOI:10.1016/S0144-8617(01)00210-7

Parab, H., Joshi, S., Sudersanan, M., Shenoy, N., Lali, A., and Sarma, U. (2010). "Removal and recovery of cobalt from aqueous solutions by adsorption using low cost lignocellulosic biomass-coir pith," *J. Environ. Sci. Health A Tox. Hazard. Subst. Environ. Eng.* 45(5), 603-611. DOI:10.1080/10934521003595662

Rana, A. K., Basak, R. K., Mitra, B. C., Lawther, M., and Banerjee, A. N. (1996). "Studies of acetylation of jute using simplified procedure and its characterization," *J. Appl. Polym. Sci.* 64(8), 1517-1523. DOI: 10.1002/(SICI)1097-4628(19970523)64:8<1517::AID-APP9>3.0.CO;2-K

Sidik, S. M., Jalil, A. A., Triwahyono, S., Adam, S. H., Satar, M. A. H., and Hameed, B. H. (2012). "Modified oil palm leaves adsorbent with enhanced hydrophobicity for crude oil removal," *Chem. Eng. J.* 203(1), 9-18. DOI:10.1016/j.cej.2012.06.132

Sun, X. F., Sun, R. C., and Sun, J. X. (2004). "Acetylation of sugarcane bagasse using NBS as a catalyst under mild reaction conditions for the production of oil sorption-active materials," *Bioresour. Technol.* 95(3), 343-350. DOI:10.1016/j.biortech.2004.02.025

Wan Ngah, W. S., and Hanafiah, M. A. K. M. (2008). "Adsorption of copper on rubber (*Hevea brasiliensis*) leaf powder: Kinetic, equilibrium and thermodynamic studies," *Biochem. Eng. J.* 39(3), 521-530. DOI:10.1016/j.bej.2007.11.006

Wang, J., Zheng, Y., and Wang, A. (2013). "Investigation of acetylated kapok fibers on the sorption of oil in water," *J. Environ. Sci.* 25(2), 246-253. DOI:10.1016/S1001-0742(12)60031-X

Warr, L. N., Perdrial, J. N., Lett, M.-C., Heinrich-Salmeron, A., and Khodja, M. (2009). "Clay mineral-enhanced bioremediation of marine oil pollution," *Appl. Clay Sci.* 46(4), 337-345. DOI:10.1016/j.clay.2009.09.012

Article submitted: December 16, 2014; Peer review completed: January 25, 2015; Revised version received and accepted: October 5, 2015; Published: October 15, 2015.
DOI: 10.15376/biores.10.4.8025-8038